

# Influences of Rice Hull in Polyurethane Foam on Its Sound Absorption Characteristics

Yonghua Wang,<sup>1,2,3</sup> Chengchun Zhang,<sup>1</sup> Luquan Ren,<sup>1</sup> Mohamed Ichchou,<sup>2</sup> Marie-Annick Galland,<sup>3</sup> Olivier Bareille<sup>2</sup>

<sup>1</sup>Key Laboratory of Bionic Engineering of Ministry of Education, Jilin University, Changchun 130025, China

<sup>2</sup>Laboratoire de Tribologie et Dynamique des Systèmes, École Centrale de Lyon, Écully 69134, France

<sup>3</sup>Laboratoire de Mécanique des Fluides et d'Acoustique, École Centrale de Lyon, Écully 69131, France

**In this article, rice hull (RH) was used in the moulding of polyurethane (PU) foam system. The article analyzed the participation of RH in the chemical reaction of PU synthesis with Attenuated Total Reflection-Fourier Transform Infrared spectroscopy method. Besides, the influence of RH on the formation of pore structure along with the acoustic performance such as sound impedance rate, acoustic reflection factor, sound absorption coefficient, and transmission loss of the products were studied with the Transfer Function Method. The results indicated that RH significantly influenced the uniformity of pore diameter in PU foam. As the content of RH increased, the sound absorption peak shifted toward lower frequency region. And the sound absorption coefficients increased till a threshold value of RH content. POLYM. COMPOS., 34:1847–1855, 2013. © 2013 Society of Plastics Engineers**

## INTRODUCTION

In recent years, rapid developments of modern industries and transportations lead to serious noise pollutions, which have significant adverse effects on the environment and personal health. One of the effective solutions in noise control is based on the use of a variety of noise reduction materials with special structures in terms of transmission route. In the last few years, new noise reduction materials have been developed with application of biomass resources as an ingredient.

---

*Correspondence to:* Chengchun Zhang; e-mail: jluzcc@jlu.edu.cn  
Contract grant sponsor: Joint Funds of the National Natural Science Foundation of China; contract grant number: U1134109; contract grant sponsor: Specialized Research Fund for the Doctoral Program of Higher Education of China; contract grant number: 20110061120048; contract grant sponsor: National Natural Science Foundation of China; contract grant numbers: 31071928, 51106062 and 51206058.  
DOI 10.1002/pc.22590  
Published online in Wiley Online Library (wileyonlinelibrary.com).  
© 2013 Society of Plastics Engineers

The natural fibers are the most attractive composite materials due to ecological and economical benefits. These composites are widely applied in packaging, building, automotive, and even aerospace industry. Numerous studies have been carried out to explore the utilization of natural fibers, including tea-leaf-fiber materials [1], ramie fiber reinforced poly composites [2], cellulose acetate biocomposites [3], polyethylene /wood flour composites [4], hemp [5], sisal [6], flax [7], jute-pp composites [8], oil palm [9], and bamboo [10]. Besides, studies are also focus on the potential of underutilized waste materials-byproducts from agricultural for industrial products. Efforts have been made to convert rice, wheat straw, corn stover, and corncobs into industrially useful products [11–13].

Polyurethane (PU) is one of the most useful three-dimensional polymers due to its unique features. It has a wide range of applications as it is light, cheap, and efficient sound insulation. PU is extensively used in acoustic and calorifuge applications because of its porous characteristics. In addition, the flexible damping characteristic of polymer foam product makes it an excellent sound-absorbing material. Mott [14] studied the acoustic and dynamic mechanical properties of a PU rubber. Scarpa [15] investigated the trends in acoustic properties of iron particle seeded auxetic PU foam. Ono [16] discussed the acoustic characteristics of unidirectionally fiber-reinforced PU foam composites for musical instrument soundboards. However, most PU belongs to polyether PU, whose biodegradation performance is very poor and may cause environmental pollution. Currently, along with the research in polyester PU, the addition of some biodegradable material is also attempted to accelerate the degradation speed of PU foam.

Modified PU foam possess various advantageous properties compared with traditional PU foam, such as low density, high stiffness, impact-proof, low thermal conductivity, low magnetic conductivity, and good damping.

TABLE 1. The physical and chemical properties of polyols.

	Hydroxyl value (mg KOH/g)	Acid value (mg KOH/g)	Moisture (%)	pH	Viscosity (mPa·s/25°C)	Molecular weight
Polyether polyol HEP-330 N	33–37	≤0.1	≤0.05	5.0–7.0	800–1000	5000
Polymer polyol TPOP-36/28	25–29	≤0.05	≤0.05	6.0–9.0	≤3500	4000

Rice Hull (RH) is a kind of agricultural waste existing widely in China, and many researchers use RH as the filler to prepare polymer complex. Rozman [17] has studied the mechanical and physical properties of PU–RH composites, while the effect of coupling agents on RH filled high-density polyethylene was studied by Panthapulakkal [18]. Deepangshu [19] has presented a review of RH filled polymeric composites. Till date, only a few investigations considered the effect of RH on the sound absorption characteristics of PU foam. In this study, PU–RH composites were fabricated to analyze their sound absorption capacity as well as the acoustic mechanism.

## MATERIALS AND METHODS

### *Synthesis of PU-RH Interconnected Porous Material*

The PU foam and PU–RH composites were fabricated by one step foaming method using polyether polyol HEP-330N, polymer polyol TPOP-36/28, deionized water, silicone oil, catalysts A33 (triethylene diamine, the concentration is 33%), and A-1 (mixture of 70% bis (2, dimethylamino ethyl) ether and 30% dipropylene glycol), modified MDI (diphenyl methane diisocyanate, the content of -NCO group is 30%). The physical and chemical properties of polyols are shown in Table 1. The proportion of each material compared with the total mass of polyols (100 fractions in all) is displayed in Table 2. The RH used in this study was obtained from Changchun Grain and oil processing. The materials for preparing PU foam were kindly supplied by Changchun Best PU.

The filler RH was dried in a baking oven at 105°C for approximately 20 h. The specific preparation process of PU foam and PU–RH composite is described in Fig. 1. The mould was kept in baking oven for more than 30 min until it reached the designed foaming temperature. The mixture was stirred for 10–15 min at high speed of 2,000 r/min with a mechanical stirrer. Poured the mixture into the mould rapidly at the cream time and postcured for 5 min. For the preparation of PU–RH composites, RH was weighed 2, 5, and 8% of the total mass of all the raw materials and then mixed with A component (all the others raw materials except modified MDI) at room temperature before mixing with B component (modified MDI).

### *Measurement Methods*

**Attenuated Total Reflection-Fourier Transform Infrared Spectroscopy (ATR-FTIR).** ATR-FTIR of PU foam and PU–RH composites was recorded on a Perkin-

Elmer spectrometer 2,000 using powder-pressed KBr pellets. FTIR spectra were obtained at a resolution of 2.0  $\text{cm}^{-1}$  at room temperature in the range of 4,000–500  $\text{cm}^{-1}$  wavenumber.

**Scanning Electron Microscope (SEM).** The foams were aged at 20°C and 50% relative humidity for 24 h before being cut for analysis. The cell size of the resultant PU foam and the morphologies of fractured surfaces of PU–RH composites were observed at room temperature by a SEM [Hitachi S-2360N, (Tokyo, Japan)]. Before testing, the samples were sliced and mounted on SEM stubs with double-sided adhesive tape, and then gold sputtered for 5 min to a thickness of about 10 nm under 0.1 torr pressure and 18 mA current to make the sample conductive. The SEM measurements were performed at an accelerating voltage of 20 kV. Micrographs were recorded at different magnifications to attain clear images.

### **Test Method for Cell Structure and Pore Diameter.**

Normally, the acoustic performance is closely related to the pore diameters of the foam. Thus, it was necessary to determine the pore diameter and its distribution. The value of pore diameter for PU foam was obtained by digital image processing software from the SEM images of foam. In this software, pixels were transformed into metric units with the purpose of obtaining the effective radius of the pores from the same areas. The values of pore diameter corresponding to the maximum normal distribution of pore diameter were obtained experimentally.

### **Test Method for Acoustic Performance.**

Four types of acoustic properties were studied: acoustic impedance, sound reflection factor, absorption coefficient, and transmission loss. They were obtained using a four-microphone impedance tube based on ISO10534-2:1998(E) [20] by Transfer Function Method. The devices we used (a), the samples (b), and the test philosophy of

TABLE 2. The formula of PU foam.

Raw materials	Weight percentage	components
Polyether polyol HEP-330N	60	A component
Polymer polyol TPOP-36/28	40	
Deionized water	2	
Silicone oil (8719)	1.8	
A33	0.6	
A-1	0.1	
Modified MDI	45	B component

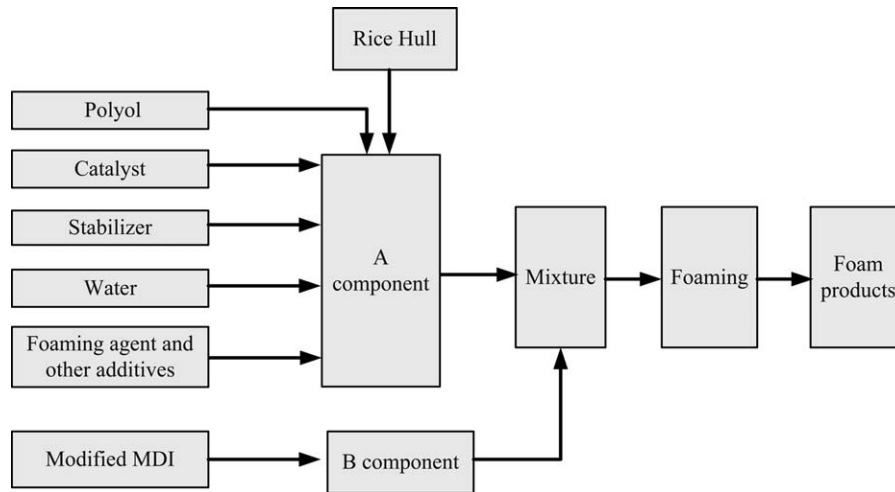


FIG. 1. Preparation process of PU foam and PU-RH composites.

sound transmission loss (c) and normal incidence absorption coefficient (d) are shown in Fig. 2. The impedance tube is manufactured by BSWA TECH. The diameter of the tube we used here is 100 mm. The type of the tube to

test absorption coefficients is SW420, which includes SW100-L (850 mm) and SW100-S (235 mm). With reference to Fig. 2, the distance between microphone 0 and 2 is 300 mm and the test frequency band is 63–500 Hz,

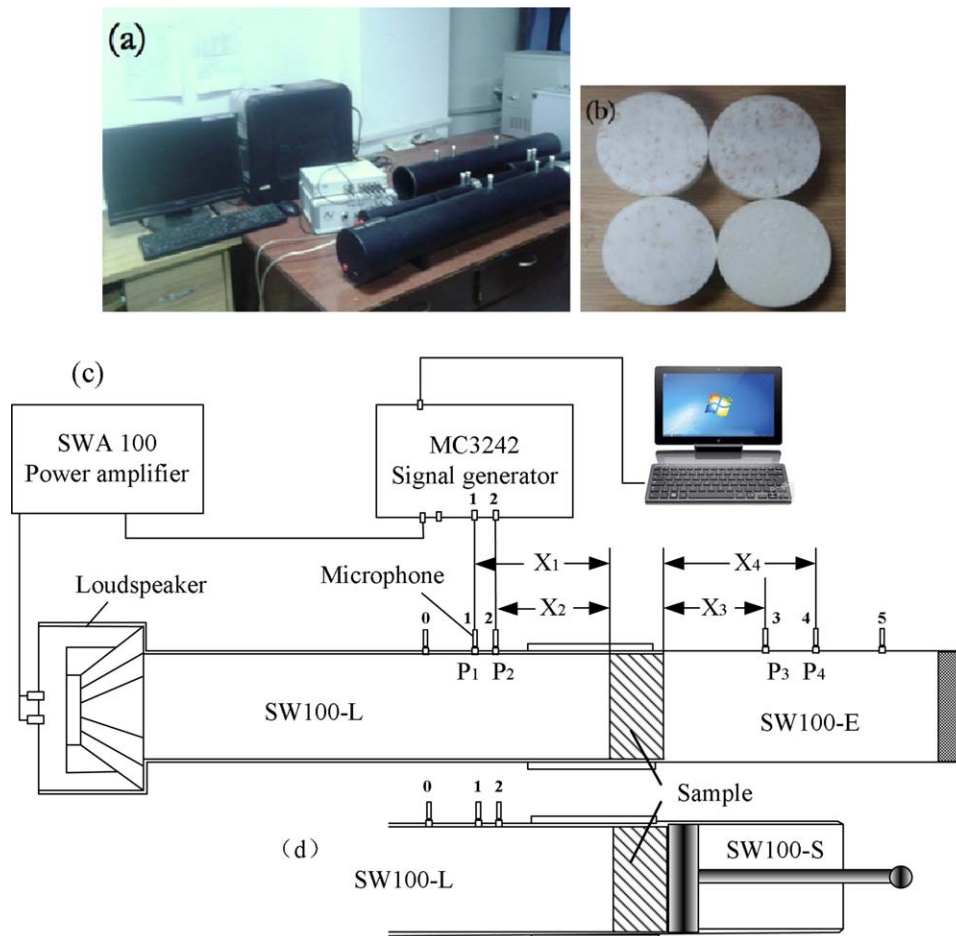


FIG. 2. The sketch map of test system of impedance tube. [Color figure can be viewed in the online issue, which is available at [wileyonlinelibrary.com](http://wileyonlinelibrary.com).]

whereas the distance between microphone 1 and 2 is 80 mm and the test frequency band is 400–1,600 Hz. The thickness between the left surface of the material and microphone 2 is 50 mm. The type of the tube to test the sound transmission loss is SW422, which includes SW100-L and SW100-E (770 mm). The distance between microphone 3 and 5 is 300 mm and that between microphone 3 and 4 is 80 mm. The thickness between the left surface of the material and microphone 3 is 150 mm. The sampling frequency of dSPACE was set at 51,200 Hz, which is high enough to avoid the aliasing problem. Broadband random sound waves were generated by the loudspeaker at one end of the impedance tube and transmitted to the surface of sample at the other end. The reflected signals were picked up by the sensors. Each sample was tailored to desired circle pieces of the thickness of 40.0 mm (Fig. 2b). The sound absorption coefficient, defined as the ratio of the acoustical energy not reflected by sample ( $I_{\text{incident}} - I_{\text{reflected}}$ ) to the acoustical incident energy ( $I_{\text{incident}}$ ) on the surface, is dependent on frequency.

The relationship between these parameters is shown as Eq. (1–4) [20,21].

$$r = \frac{P_2 + e^{-jk(X_1 - X_2)} P_1}{P_1 e^{jk(X_1 - X_2)} - P_2} e^{2jkX_1} \quad (1)$$

$$Z_s = [(1+r)/(1-r)] \rho_0 c_0 \quad (2)$$

$$\alpha = 1 - |r|^2 \quad (3)$$

$$TL = -20 \lg \left( \frac{\sin [k(X_1 - X_2)]}{\sin [k(X_4 - X_3)]} \times \frac{P_3 e^{jk(X_4 - X_3)} - P_4}{P_1 - P_2 e^{-jk(X_1 - X_2)}} \times e^{jk(X_2 + X_3)} \right) \quad (4)$$

Where  $X_1, X_2, X_3, X_4$  are the distances of the microphones and the surface of the test sample, respectively;  $p_2, p_3, p_3, p_4$  are the complex sound pressures at the corresponding positions, respectively;  $k$  is the complex wave-number;  $Z_s$  is the acoustic impedance;  $r$  is the sound reflection factor;  $\alpha$  is the sound absorption coefficient;  $TL$  is the transmission loss;  $\rho_0$  and  $c_0$  are the density of air and the speed of sound, respectively.

The incident sound was perpendicular to the surface of the foam rise direction. Each of the tests was repeated with at least five samples to obtain consistent and representative results, and made at the temperature of  $20 \pm 2^\circ\text{C}$  and relative humidity of  $60 \pm 10\%$ .

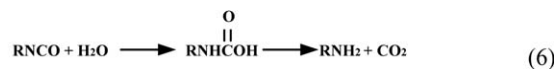
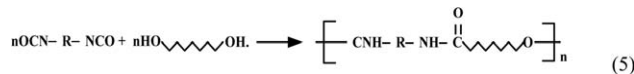
## RESULTS AND DISCUSSION

### The Results of ATR-FTIR

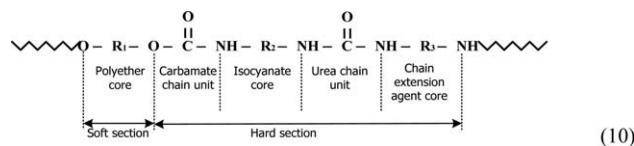
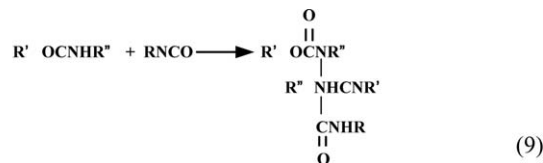
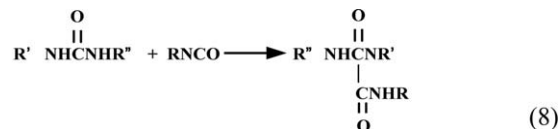
The content of -NCO group must be appropriate according to the designation of PU chains. Free-rise PU foams were obtained from the simultaneous reaction of

polyisocyanate with polyols and water. The reaction process is listed below.

During the initial extender chain reaction, isocyanate groups reacted with hydroxyl groups of polyol to form the PU chains. The end of extender chain reaction was isocyanate group. Subsequently in the foaming reaction, isocyanate groups reacted with water to form an amino acid group which was unstable and dissociated into a chain with amine end-group and carbon dioxide. The extent of  $\text{CO}_2$  by this reaction contributed significantly to the porosity. Finally, a chain with amine end-group reacted with an isocyanate end-group to form a urea linkage. As expressed in Eq. (5–7).



However, the polymer structure must build up rapidly to support the fragile foam in order to form a stable cellular structure, but not be fast to restrict bubble growth. These following competing reactions were balanced by the addition of catalysts and foam stabilizer: (1) formation of biuret on addition of water as blowing agent, urea bond compound gets generated, and subsequently reacted with excess isocyanate at high temperature to form biuret bond compound (Eq. 8); (2) formation of allophanate-hydrogen bond of carbamate reacted with excess isocyanate and produce allophanate bond at high temperature (Eq. 9). Finally, block polymer was developed as shown in Eq. (10).



The FTIR spectra of PU foam and PU–RH composites are shown in Fig. 3. The characteristic peaks of PU were found in the curves of both PU foam and PU–RH



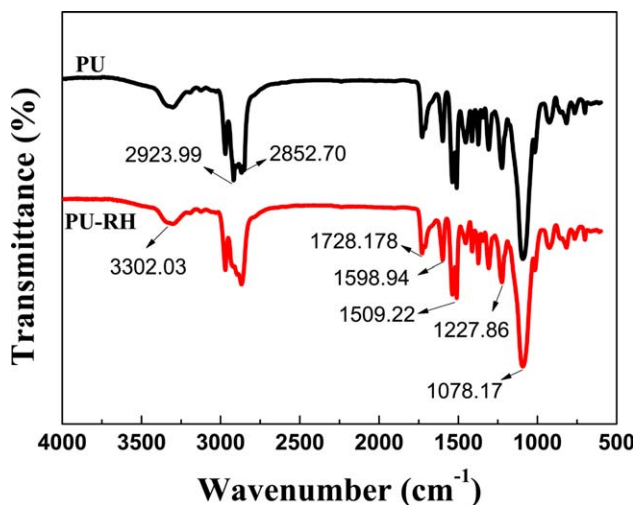


FIG. 3. ATR-FTIR spectra of PU and PU-RH composites. [Color figure can be viewed in the online issue, which is available at [wileyonlinelibrary.com](http://wileyonlinelibrary.com).]

composites. The peak located at about  $3,300\text{ cm}^{-1}$  was due to stretching vibration of N—H group of urethane linkages. The peak at about  $2,923$  and  $2,852\text{ cm}^{-1}$  correspond to the nonsymmetric and symmetric stretching vibration of  $\text{CH}_2$ , respectively. The peaks at about  $1,728$ ,  $1,227$ , and  $1,078\text{ cm}^{-1}$  were due to the stretching vibration of C—O, the stretching vibration of aromatic C—O, and the nonsymmetric stretching vibration of C—O—C, respectively [22]. The absorption near  $1,509\text{ cm}^{-1}$  can be attributed to the bending vibration of N—H and stretching vibration of C—N. Fig. 3 showed that the change trends of absorbance curves of PU foam and PU-RH composites were very consistent. They had almost the same absorption peaks, which proved that RH did not participate in the chemical reaction of PU synthesis.

#### Porous Cell Morphologies and Cell Size Distribution

**Porous Cell Morphologies.** The interconnected porosity is an important parameter governing the acoustic behavior of polymer porous materials. In order to study the acoustic performance, the interconnected porous cell network must be taken regard. The open porous cell morphology of PU foam (one same sample) is shown in Fig. 4. The white part corresponded to the pore shape while the dark part was related to the open holes. The typical porous structure was distinct and the distribution of cells was relatively uniform. Almost all the pores were open pores and connected. The frames between the pores were triangular in shape. Results indicated that the compound of A-1 and A33 at the ratio of 0.1:0.6 as catalysts along with foam stabilizer-silicone oil 8,971 can control the foam size distribution and they were in favour of the open porous cells under the blowing agent. The reaction between the polyols and modified MDI produced a network. For the water-based PU, the polyisocyanate was blocked to reduce its chemical reactivity as the

hydrophobic ethyl group provided hydrolytic stability. However, the presence of moisture broke part of the blocking structure to release  $\text{CO}_2$ . At high degree of reticulation, the pores formed by released  $\text{CO}_2$  were interconnected due to a coordination of the foam blowing time with the PU polymer gel time.

Some SEM micrographs of PU-RH composites are shown in Fig. 5 (Fig. 5a–c came from one sample whereas Fig. 5d–f came from another sample). The figure indicated that the pore structure was significantly different from PU foam. The distribution of cells in PU-RH composites was nonuniform. The pores in the vicinity of RH were much smaller compared to the areas without RH (Fig. 5a and b). This indicated that the presence of RH reduced the formation of pores in the PU-RH composites. However, in the PU-RH composites, the diameter of pores in the area where RH was not present was larger as compared to PU foam. And the results clearly indicated the presence

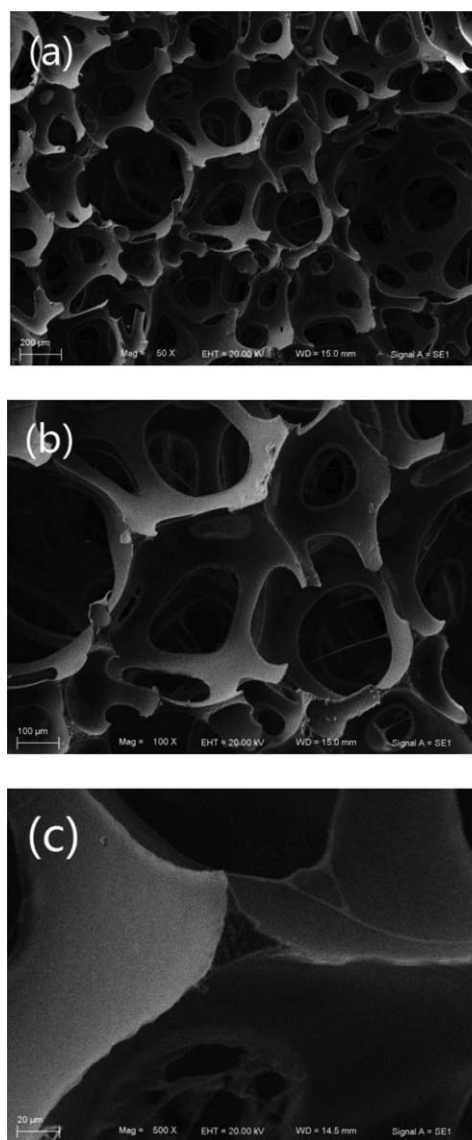


FIG. 4. Some SEM micrographs of PU foam.

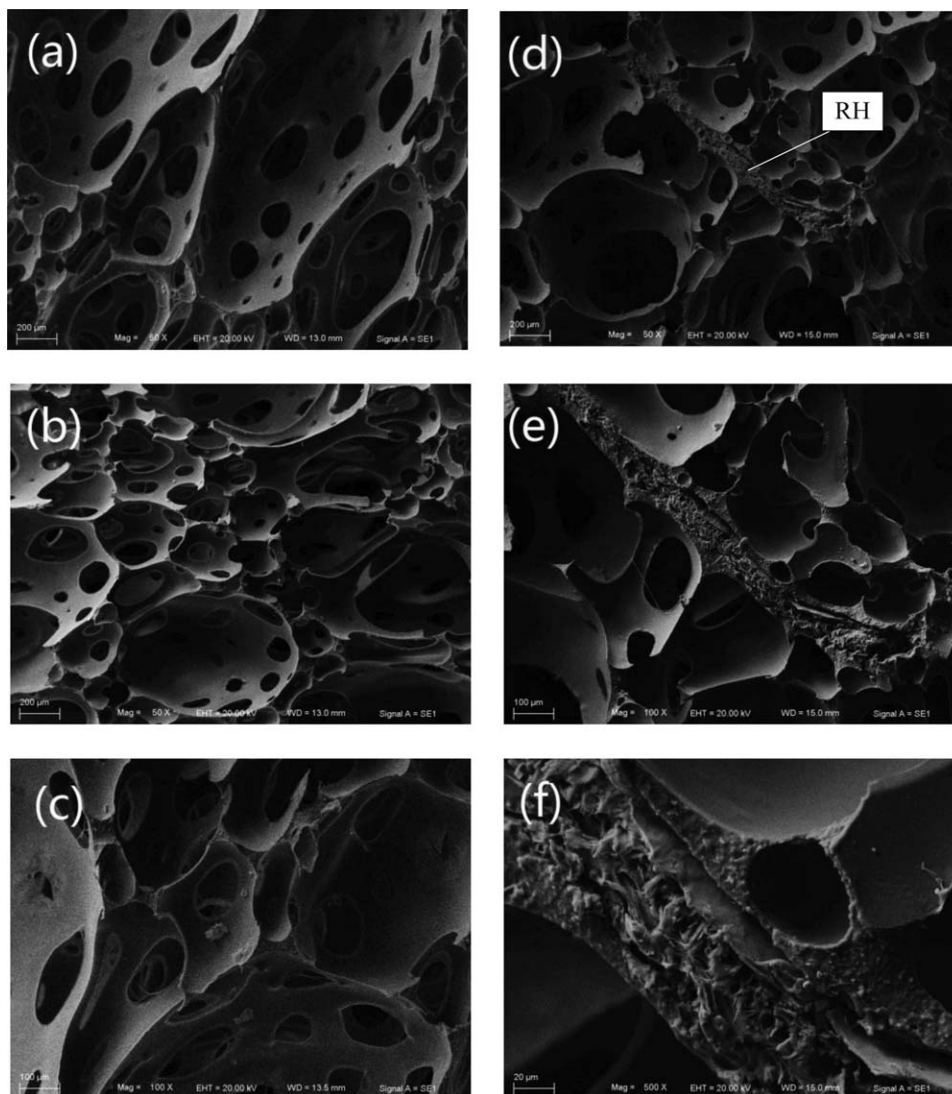


FIG. 5. Some SEM micrographs of PU-RH composites.

of typical RH fiber morphology between two zones of PU-RH composites.

**Cell Size Distribution and Pore Diameter.** The pore diameter is another important parameter to govern the acoustic behavior. The value of pore diameter corresponds to maximum normal distribution of pore diameter obtained experimentally by the digital image processing method. The maximum pore diameter was found to be 0.10 mm from the probability distribution for PU foam (Fig. 6).

#### *The Results of Acoustic Performance*

**Acoustic Impedance.** The acoustic measurements of PU foam and PU-RH composites with varying RH contents of 2%, 5%, and 8% were studied at the low frequency range from 50 Hz up to 1,600 Hz. The real part

and imaginary part of acoustic impedance ratio of various foams are shown in Fig. 7. The results indicated that:

1. The curves of acoustic impedances of PU-RH composites had the same trend with PU foam. Two distinct peaks were observed at 310 and 515 Hz in the plot for the real part of acoustic impedance while small variations were observed between 900 and 1,400 Hz. No significant change in impedance values were observed for the addition of smaller percentage of RH (2%) in PU foam. In case of all the curves at about 310 Hz, the maximum value of impedance reduced from 7,600 for 2% PU-RH composite (6,400 for PU foam) to 4,300 for 8% PU-RH composite. Similar trends were observed in case of the peak at 515 Hz. Indicating that the addition of RH reduced the impedance in PU foam. And in case of higher frequency (above 900 Hz), the impedance values for both PU foam and 2% PU-RH composite remained constant. However, 8% PU-RH composite showed higher value (1,248) at 1,230 Hz.

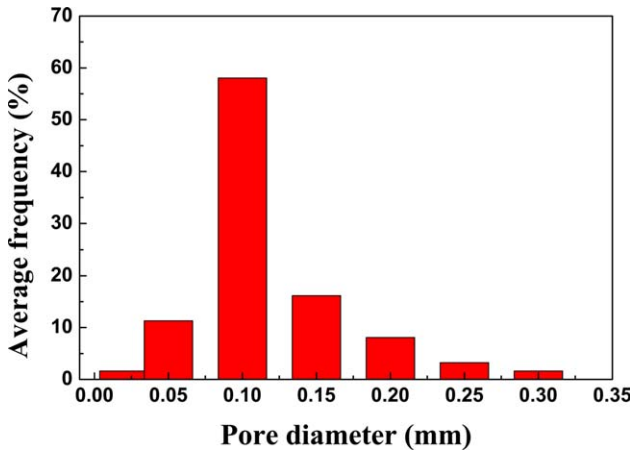


FIG. 6. Pore diameter distribution of PU foam. [Color figure can be viewed in the online issue, which is available at [wileyonlinelibrary.com](http://wileyonlinelibrary.com).]

2. In case of imaginary part of acoustic impedance, the results revealed identical fluctuations in both positive and negative zones till 650 Hz. In this range, four peaks were observed at 303, 316, 505, and 540 Hz, respectively. The trends of four curves were similar to that observed for

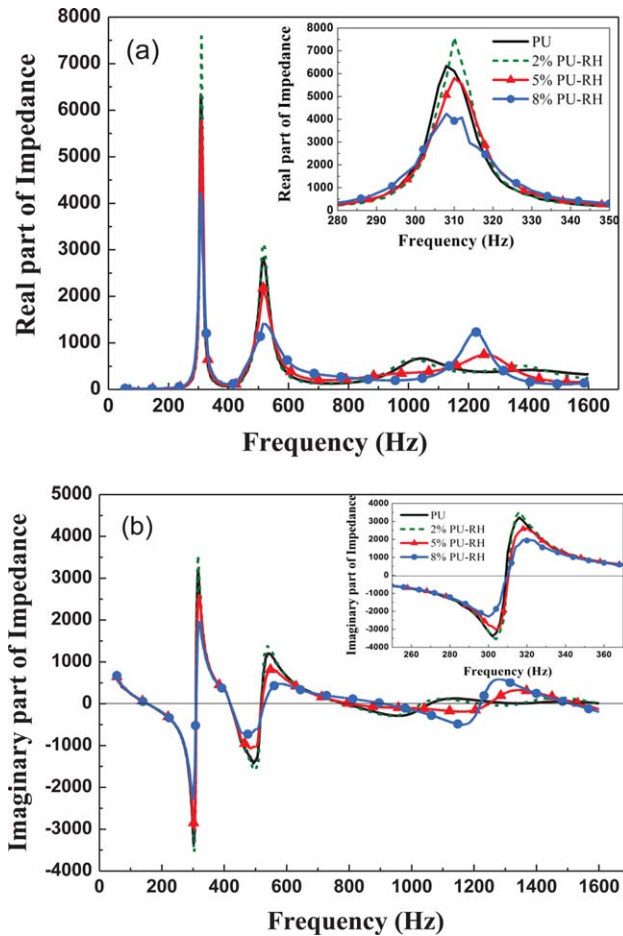


FIG. 7. The real part (a) and the imaginary part (b) of impedance for various foams. [Color figure can be viewed in the online issue, which is available at [wileyonlinelibrary.com](http://wileyonlinelibrary.com).]

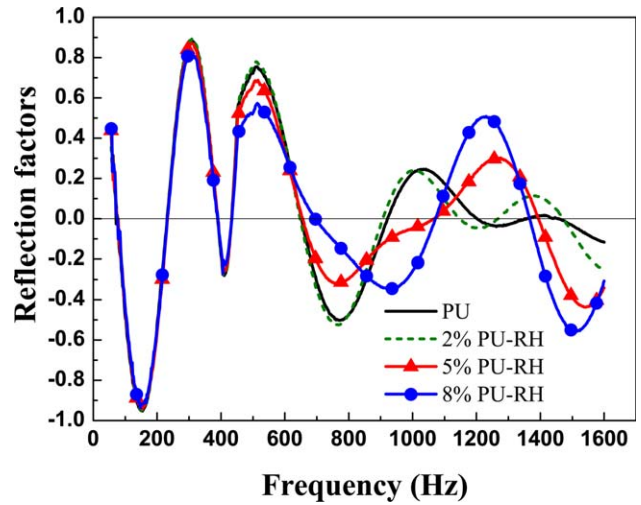


FIG. 8. The reflection factor of various foams. [Color figure can be viewed in the online issue, which is available at [wileyonlinelibrary.com](http://wileyonlinelibrary.com).]

real parts, wherein PU foam and 2% PU–RH composite had higher impedance as compared to PU–RH composite with 5 and 8% RH. Beyond 900 Hz, there were variations in impedance values with 8% PU–RH composite, showing maximum values.

**Sound Reflection Factor.** The reflection factors of different foams are shown in Fig. 8. The curves showed both positive and negative variations. The results indicated that the values of reflection factor were almost same till low frequency of 400 Hz. However, in the zone between 400 and 620 Hz, the reflection factor for PU foam and 2% PU–RH composite was found to be higher as compared to 5 and 8% PU–RH composites. In case of higher frequency (above 620 Hz), 8% PU–RH composite showed higher values of reflection factor.

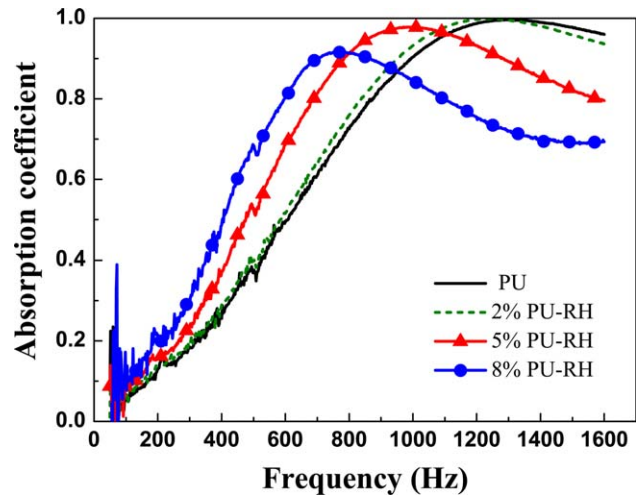


FIG. 9. The sound absorption coefficient of various foams. [Color figure can be viewed in the online issue, which is available at [wileyonlinelibrary.com](http://wileyonlinelibrary.com).]



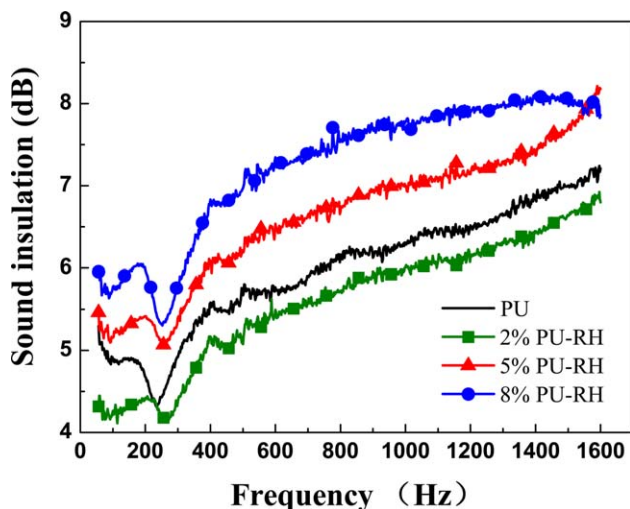


FIG. 10. The sound transmission losses of various foams. [Color figure can be viewed in the online issue, which is available at [wileyonlinelibrary.com](http://wileyonlinelibrary.com).]

**Sound Absorption Coefficient.** The sound absorption coefficients of various foams are shown in Fig. 9. The results indicated that:

1. The sound absorption curves of PU foam and PU–RH composites were in accordance with that of typical porous material. The sound absorption coefficient increased continuously in the low frequency and fluctuations appeared with different degrees in high frequency.
2. The acoustic absorption of the system improved almost over the entire frequency range, especially at the low frequency (50–1,000 Hz) due to the addition of RH. In the frequency range from 50 to 1,000 Hz, the average sound absorption coefficient of PU foam, PU–RH composites with 2% RH, 5% RH and with 8% RH was 0.435, 0.454, 0.55, and 0.599, respectively.
3. The maximum absorption coefficient of 0.996 appeared at 1,300 Hz for PU foam, indicating complete absorption of sound. However, the value of 0.93 was achieved by PU–RH composite of 8% for low frequency. Thus addition of significant amount of RH enhanced the sound absorption coefficient of PU foam in low frequency. In general, the results indicated that PU–RH composite of 5% RH can be considered to provide the most satisfactory sound absorption coefficient in comparison with others foams.

**Sound Transmission Loss.** The sound transmission losses of different foams are shown in Fig. 10. The results indicated that the curves had the similar trends. There was a steady increase in sound transmission loss for all the foams along with the frequency increasing on the whole. However, a striking reduction was located at about 250 Hz. The sound insulation performance was opposite compared with the sound absorption coefficient. The better the sound absorption coefficient of the material was, the poorer the sound insulation performance would be. The results revealed that PU–RH composite of 8% RH has the best sound insulation characteristics.

### Sound Absorption Mechanism

Theoretically, the sound absorption properties of a porous medium were mainly influenced by its porous cell size, structure, and distribution as well as the acoustic impedance of the material. The results suggested improvement in sound absorption of PU foam due to the addition of RH. The sound absorption mechanisms of PU–RH composites can be drawn as follows:

1. The sound absorption performance of polymer porous foam depends on the orientation/network of pores and vibroacoustic energy carried by air in the pores as well as solid frame structure. Sound is primarily dissipated due to viscous flow, thermal damping, and Helmholtz resonance effect. In case of PU foam, sound absorption coefficient is higher for larger cells as compared to small ones of a given frequency. Some of the mechanical-acoustical energy is dissipated into heat due to the difference in amplitude and phase. In case of PU–RH composites, mechanical and viscoacoustic phenomena take place in the solid frame, interface between solid frame and air in the pores as well as solid frame and RH. In case of pressure or disturbance from sound wave, energy in the porous cell is converted into heat due to frictional force between the air flow and cell wall. During the above process, the cells are forced to stretch, bend and buckle, generating kinetic energy. The addition of RH will cause nonuniform distribution of pores in the foam along with large pore size. The wave of low frequency can then be sufficiently absorbed by these large pores. The larger pores of PU–RH composites contain more air and can produce more frictional heat from sound energy than PU foam energy [23]. Additionally, the RH at interface forces more amount of sound energy to be dissipated to kinetic energy, causing foam to stretch, bend and buckle. Thus the sound absorption coefficients of PU foam substantially increase due to the addition of significant amount of RH.
2. The enhancement of sound absorption coefficient was also observed for low frequency in PU–RH composites. Increase in sound absorption of PU–RH composites in comparison to PU foam with the same volume results from the fact that incident plane wave at low frequency are converted to higher-order symmetric modes within the interfaces of PU frame and RH [24,25].
3. RH is a natural fiber which has good sound absorption performance. PU–RH composites combine sound absorption performance of both PU foam as well as RH. The composites have more fine pores, increasing the chance to interfere with the sound wave. This improves the resistance through the vibration of air by means of frictional viscosity [26].
4. For PU foam, almost all the pores are interconnected between each other. On addition of RH into PU foam, the connected pores are blocked. Sound waves would reflect when it meets RH in its propagation path, thus extending the transmission route in the foam. There is an increase in energy loss due to transmission. This leads to increase in the sound absorption coefficient, especially in low frequency.



## CONCLUSIONS

In this study, the sound absorption tests were performed for PU foam and PU–RH composites with different content of RH. The absorption performance of PU foam is not very satisfying at low frequency while it is excellent at high frequency. It almost reaches 1 when the frequency is higher than 1,200 Hz, however, it is less than 0.3 under 500 Hz. On addition of RH into PU, the sound absorption coefficients increase at low frequency along with small decrease at high frequency. It should be noted that it is difficult to improve the sound absorption performance at low frequency without increasing the thickness of the material. The pore cell morphologies and sound absorption performance for PU foam were investigated, so as to study the mechanism of the change of sound absorption capacity. Further investigations could lead to better absorbing systems for practical application. In addition, as an agriculture waste, RH is sure to meet sustainable development requirements. Furthermore, adding RH improves biodegradation of the foam composites, which is one of the most important requirements of green material. These advantages make PU–RH a kind of attractive candidate for many applications in noise control of automobiles, aerospace industry, and construction industry.

## ACKNOWLEDGMENT

All support is greatly acknowledged and appreciated, especially the constructive discussion and criticism from colleagues. Thanks to Changchun Best PU for providing the material.

## REFERENCES

1. E. Sezgin and K. Haluk, *Appl. Acoust.*, **70**(1), 215 (2009).
2. D. Chen, J. Li, and J. Ren., Study on sound absorption property of ramie fiber reinforced poly (L-lactic acid) composites: Morphology and properties. *Compos. Part A:Appl. Sci. Manuf.*, **41**(8), 1012 (2010).
3. A.K. Mohanty, A. Wibowo, M. Misra, and L.T. Drzal, *Compos. A*, **35**, 363 (2004).
4. M. Bengtsson, P. Gatenholm, and K. Oksman, *Compos. Sci. Technol.*, **65**, 1468 (2005).
5. B.M. Prasad and M.M. Sain, *Mater. Res. Innovations*, **7**, 231 (2003).
6. Y. Li, Y.W. Mai, and L. Ye, *Compos. Sci. Technol.*, **60**, 2037 (2000).
7. V.K. Vande and P. Keikens, *Polym. Test*, **20**, 885 (2001).
8. C.K. Honga, I. Hwangb, N. Kimb, D.H. Parkc, B.S. Hwangd, and C. Nahb, *J. Ind. Eng. Chem.*, **14**(1), 71 (2008).
9. M.S. Sreekala, J. George, M.G. Kumaran, and S. Thomas, *Compos. Sci. Technol.*, **62**, 339 (2002).
10. X.Y. Chen, Q.P. Guo, and X.L. Mi, *J. Appl. Polym. Sci.*, **69**, 1891 (1998).
11. D.H. Wang and X.S. Sun, *Ind Crops Prod.*, **15**, 43 (2002).
12. H.S. Yang, D.J. Kim, and H.J. Kim, *Bioresour. Technol.*, **86**, 117 (2003).
13. W.T. Tsai, C.Y. Chang, and S.L. Lee, *Bioresour. Technol.*, **64**, 211 (1998).
14. P.H. Mott, C.M. Roland, and R.D. Corsaro, *J. Acoust. Soc. Am.*, **111**, 1782 (2002).
15. F. Scarpa, W.A. Bullough, and P. Lumley. Trends in acoustic properties of iron particle seeded auxetic polyurethane foam. *Proc. Inst. Mech. Eng., Part C: J. Mech. Eng. Sci.*, **218**(2), 241 (2004).
16. T. Ono, S. Miyakoshi, and U. Watanabe, *Acoust. Sci. Technol.*, **23**(3), 135 (2002).
17. H.D. Rozman, Y.S. Yeo, G.S. Tay, and A. Abubakar, *Polym. Testing*, **22**, 617 (2003).
18. S. Panthapulakkal, M. Sain, and S. Law, *Polym. Int.*, **54**, 137 (2005).
19. D.S. Chaudhary, M.C. Jollands, and F. Cser, *Adv. Polym. Technol.*, **23**(2), 147 (2004).
20. European Committee for Standardization (CEN), "Acoustics-determination of sound absorption coefficient and impedance in impedances tubes-Part 2: transfer-function method," ISO10534-2, CEN, Brussels, Belgium (1998).
21. B. Qu and B.L. Zhu, *Noise Vib. Control*, **12**, 44 (2002).
22. X.M. Zhang, R.J. Xu, Z.G. Wu, and C.X. Zhou, *Polym. Int.*, **52**, 790 (2003).
23. E.L. Nordgren and P. Goransson, *J. Sound Vib.*, **329**, 753 (2010).
24. X. Yang, Y.S. Wang, and H.W. Yu, *Mater. Manuf. Processes*, **22**, 721 (2007).
25. W.H. Chen, F.C. Lee, and D.M. Chiang, *J. Sound Vib.*, **237**(2), 337 (2000).
26. Y. Lee and C. Joo, *AUTEX Res. J.*, **3**(2), 83 (2003).